



# Diverse Properties of Molecular Gas in the Host Galaxies of Fast Radio Bursts

Bunyo Hatsukade<sup>1</sup>, Tetsuya Hashimoto<sup>2</sup>, Yuu Niino<sup>1,3</sup>, and Tzu-Yin Hsu<sup>4</sup>

<sup>1</sup>Institute of Astronomy, Graduate School of Science, The University of Tokyo, 2-21-1 Osawa, Mitaka, Tokyo 181-0015, Japan; [hatsukade@ioa.s.u-tokyo.ac.jp](mailto:hatsukade@ioa.s.u-tokyo.ac.jp)

<sup>2</sup>Department of Physics, National Chung Hsing University, No. 145, Xingda Road, South Dist., Taichung, 40227, Taiwan (R.O.C.)

<sup>3</sup>Research Center for the Early Universe, The University of Tokyo, 7-3-1 Hongo, Bunkyo, Tokyo 113-0033, Japan

<sup>4</sup>Department of Physics, National Tsing Hua University, 101, Section 2, Kuang-Fu Road, Hsinchu, 30013, Taiwan (R.O.C.)

Received 2022 August 28; revised 2022 October 19; accepted 2022 November 1; published 2022 November 28

## Abstract

We report the properties of molecular gas in a sample of six host galaxies of fast radio bursts (FRBs) obtained from CO observations with the Atacama Large Millimeter/submillimeter Array (FRBs 20180924B, 20190102C, and 20190711A), the results of one nondetection in a dwarf galaxy (FRB 20121102A), and two events detected in M81 (FRB 20200120E) and the Milky Way (FRB 20200428A). The CO observations resulted in the detection of CO(3–2) emission in the FRB 20180924B host and nondetections of CO(3–2) and CO(2–1) emission in the hosts of FRB 20190102C and FRB 20190711A, respectively. The derived molecular gas mass and  $3\sigma$  upper limit is  $(2.4 \pm 0.2) \times 10^9 M_\odot$ ,  $<3.8 \times 10^8 M_\odot$ , and  $<6.7 \times 10^9 M_\odot$  for the hosts of FRB 20180924B, FRB 20190102C, and FRB 20190711A, respectively. We found diversity in molecular gas properties (gas mass, gas depletion time, and gas fraction to stellar mass) in the sample. Compared to other star-forming galaxies, the FRB 20180924B host is gas-rich (the larger molecular gas fraction), and the hosts of FRB 20190102C and FRB 20200120E are gas-poor with a shorter depletion time for their stellar mass and star formation rate. Our findings suggest that FRBs arise from multiple progenitors or single progenitors that can exist in a wide range of galaxy environments. Statistical analysis shows a significant difference in the distribution of molecular gas fraction between the FRB hosts and local star-forming galaxies. However, the difference is not substantial when an outlier, the FRB 20200120E host, is excluded, and analysis with a larger sample is needed.

*Unified Astronomy Thesaurus concepts:* Radio transient sources (2008); Extragalactic radio sources (508); Radio bursts (1339); Galaxies (573); CO line emission (262); Molecular gas (1073); Interstellar medium (847); Star formation (1569); Radio astronomy (1338); Radio interferometry (1346); Observational astronomy (1145)

## 1. Introduction

Fast radio bursts (FRBs) are bright, energetic radio pulses with a duration of microseconds to milliseconds (see Cordes & Chatterjee 2019 for a review). FRBs' physical mechanism and progenitors are one of the biggest mysteries of modern astronomy. FRBs are now thought to be extragalactic phenomena because of their large dispersion measures (e.g., Cordes & Chatterjee 2019) together with the identifications of extragalactic host galaxies (e.g., Heintz et al. 2020). FRBs are classified into repeating bursts and (apparently) nonrepeating (one-off) bursts. It is highly debated whether the two types of FRBs are the same population or not (e.g., Hashimoto et al. 2020; Pleunis et al. 2021). Many theoretical models have been proposed to explain FRBs (Platts et al. 2019). Recently, a millisecond-duration radio burst (FRB 20200428A) was detected from the Galactic magnetar SGR 1935+2154 (Bochenek et al. 2020; The CHIME/FRB Collaboration et al. 2020), suggesting a magnetar origin of other extragalactic FRBs.

Because the link between progenitors and specific galactic environments is expected, observations of host galaxies are essential to understand their nature and constrain models, as demonstrated by studies of astronomical transients such as gamma-ray bursts (GRBs; e.g., Le Floch et al. 2006; Perley et al. 2016; Niino et al. 2017; Hashimoto et al. 2019). Only recently, new facilities and extensive follow-up campaigns

have enabled localization of FRBs and identifications of host galaxies (e.g., Chatterjee et al. 2017; Bannister et al. 2019; Prochaska et al. 2019; Macquart et al. 2020; Marcote et al. 2020). Optical/near-infrared observations show that the hosts span a wide range of morphology, color, stellar mass, and star formation rate (SFR) (e.g., Heintz et al. 2020; Bhandari et al. 2022). Comparison with the hosts of other transients suggested that the generally massive and metal-rich environments of FRBs disfavor similar progenitor formation channels to those of long-duration GRBs (LGRBs) and superluminous supernovae (SLSNe) (e.g., Li et al. 2019; Bhandari et al. 2020; Heintz et al. 2020; Li & Zhang 2020).

CO observations of host galaxies provide physical properties of the interstellar medium as a material for star formation in the environment of FRBs, such as molecular gas content, gas depletion time, gas fraction, and star formation efficiency. Bower et al. (2018) conducted Submillimeter Array and Northern Extended Millimeter Array observations of the host galaxy of FRB 20121102A in the CO(3–2) and CO(1–0) transitions, respectively, and did not detect emission from either transition.

In this Letter, we present molecular gas observations in the host galaxies of three FRBs (20180924B, 20190102C, and 20190711A) performed with the Atacama Large Millimeter/submillimeter Array (ALMA). Adding the other three host galaxies of FRBs (20121102A, 20200120E, and 20200428A) for which molecular gas data are available in the literature, we discuss the properties of molecular gas in the six host galaxies. Section 2 describes ALMA observations of the FRB host galaxies, data reduction, and results. In Section 3, we derive the



Original content from this work may be used under the terms of the [Creative Commons Attribution 4.0 licence](https://creativecommons.org/licenses/by/4.0/). Any further distribution of this work must maintain attribution to the author(s) and the title of the work, journal citation and DOI.

physical properties of molecular gas in the FRB hosts, compare them with those of other galaxy populations, and discuss environments where FRB progenitors originate. Conclusions and implications for progenitors are presented in Section 4. Throughout the paper, we adopt a Chabrier (2003) initial mass function and cosmological parameters of  $H_0 = 67.7 \text{ km s}^{-1} \text{ Mpc}^{-1}$  and  $\Omega_M = 0.310$  based on the Planck 2018 results (Planck Collaboration et al. 2020).

## 2. ALMA Data

### 2.1. Target Host Galaxies

FRB 20180924B was detected on 2018 September 24 at 16:23:12.6265 UTC with the Australian Square Kilometre Array Pathfinder (ASKAP; Johnston et al. 2008) and was localized to a host galaxy at  $z = 0.3214$ , DES J214425.25–405400.81 (Bannister et al. 2019). The host has a stellar mass of  $M_* = (13.2 \pm 5.1) \times 10^9 M_\odot$ , an SFR of  $0.88 \pm 0.26 M_\odot \text{ yr}^{-1}$ , and a gas-phase metallicity of  $12 + \log(\text{O}/\text{H}) = 8.93^{+0.02}_{-0.02}$  (Heintz et al. 2020). It is located between star-forming and quiescent galaxies (“green valley”) in a color–magnitude diagram and an SFR– $M_*$  plot (Heintz et al. 2020). A Baldwin–Phillips–Terlevich (BPT) diagram (Baldwin et al. 1981) shows that the host has the characteristic of a low-ionization narrow-emission-line region (Bannister et al. 2019).

FRB 20190102C was detected on 2019 January 2 at 05:38:43.49184 UTC with ASKAP and was localized to a host galaxy at  $z = 0.291$  (Macquart et al. 2020). The host has a stellar mass of  $(3.39 \pm 1.02) \times 10^9 M_\odot$ , an SFR of  $0.86 \pm 0.26 M_\odot \text{ yr}^{-1}$ , and a metallicity of  $12 + \log(\text{O}/\text{H}) = 8.70^{+0.08}_{-0.07}$  (Heintz et al. 2020). The host is located in the “composite” region close to the boundary of star-forming galaxies and active galactic nuclei on the BPT diagram (Bhandari et al. 2020).

FRB 20190711A was detected on 2019 July 11 at 01:53:41.09338 UTC with ASKAP and was localized to a host galaxy at  $z = 0.5220$  (Macquart et al. 2020). The host galaxy is a typical star-forming galaxy at its redshift with the stellar mass of  $(0.81 \pm 0.29) \times 10^9 M_\odot$  and an SFR of  $0.42 \pm 0.12 M_\odot \text{ yr}^{-1}$  (Heintz et al. 2020).

### 2.2. Observations and Data Reduction

We conducted ALMA Band 4 CO(2–1) observations of the FRB 20190711A host from 2022 May 2 to June 9 (project code: 2021.1.00027.S). The correlator was used in the time-domain mode with a bandwidth of 1.875 GHz ( $488.28 \text{ kHz} \times 3840$  channels). Four basebands were used, providing a total bandwidth of 7.5 GHz. The array configuration was C-3 and C-4 with the baseline lengths of 15.1–500.2 and 15.1–783.5 m, respectively. The number of the available antennas was 41–46, and the on-source integration time was 6.95 hr. Bandpass and flux calibrations were performed with J2357–5311 and phase calibrations with J2116–8053.

We utilized the ALMA archive data of Band 6 CO(3–2) observations of the hosts of FRBs 20180924B and 20190102C (project code: 2019.1.01450.S).<sup>5</sup> Observations of the FRB 20180924B host were conducted on 2019 November 26, using 44–46 antennas in an array configuration with baseline lengths of 15.0–313.7 m. The correlator setup consists of a baseband with the bandwidth of 1.875 GHz

(7812.5 MHz  $\times$  240 channels) for the CO line and three basebands with a bandwidth of 2 GHz ( $15.625 \text{ MHz} \times 128$  channels) for the continuum. The on-source integration time was 27 minutes. Observations of the FRB 20190102C host were conducted on 2019 November 30 and December 3, using 40–43 antennas in an array configuration with baseline lengths of 15.1–312.7 m. The same correlator setup was used for the FRB 20180924B host observations. The on-source integration time was 88 minutes.

The data were reduced with Common Astronomy Software Applications (CASA; McMullin et al. 2007). Data calibration was done with the ALMA Science Pipeline Software of CASA. Maps were processed with a `tclean` task with Briggs weighting and a `robust` parameter of 2.0. A clean box was placed for imaging the CO emission of the FRB 20180924B host, where a component with a peak signal-to-noise ratio (S/N) above 5 was identified. The continuum maps were created by excluding channels with CO emission. The rms noise level of the CO maps is 34, 340, and  $67 \mu\text{Jy beam}^{-1}$  with a velocity resolution of  $50 \text{ km s}^{-1}$  for the hosts of FRBs 20180924B, 20190102C, and 20190711A, respectively. The rms noise level of the continuum maps is 47, 56, and  $3.8 \mu\text{Jy beam}^{-1}$ .

### 2.3. Results

Figure 1 shows CO spectrum, velocity-integrated CO maps, and continuum maps. The CO(3–2) emission is significantly detected in the FRB 20180924B host with a peak S/N of 12 in the velocity-integrated intensity map. The emission is spatially unresolved with the synthesized beam. The peak position of the CO emission coincides with the host-galaxy center. The CO spectra shows a full width at zero intensity of  $\sim 400 \text{ km s}^{-1}$  and an FWHM of  $\sim 270 \text{ km s}^{-1}$ , which is comparable to those of local star-forming galaxies with  $M_* > 10^{10} M_\odot$  (Saintonge et al. 2017). In the FRB 20190711A host spectrum, there is a feature of emission at  $200\text{--}400 \text{ km s}^{-1}$ . Although the peak position of the velocity-integrated intensity map coincides with the host-galaxy center, the feature is marginal (S/N = 3.3). There is also a  $3.1\sigma$  signal in the continuum map of the FRB 20190711A host, although the peak position is  $\sim 0''.6$  away from the host-galaxy center. Except for the CO emission in the FRB 20180924B host, we do not find significant emission in the CO line and continuum maps.

## 3. Discussion

### 3.1. Molecular Gas Mass

We derive molecular gas mass from the results of CO observations. The CO luminosity is calculated as follows (Solomon & Vanden Bout 2005),

$$L'_{\text{CO}} = 3.25 \times 10^7 S_{\text{CO}} \Delta v \nu_{\text{obs}}^{-2} D_L^2 (1+z)^{-3}, \quad (1)$$

where  $L'_{\text{CO}}$  is in  $\text{K km s}^{-1} \text{ pc}^2$ ,  $S_{\text{CO}} \Delta v$  is the velocity-integrated intensity in  $\text{Jy km s}^{-1}$ ,  $\nu_{\text{obs}}$  is the observed line frequency in GHz, and  $D_L$  is the luminosity distance in megaparsecs. The molecular gas mass is derived from

$$M_{\text{gas}} = \alpha_{\text{CO}} L'_{\text{CO}(1-0)}. \quad (2)$$

The CO(1–0) luminosity,  $L'_{\text{CO}(1-0)}$ , is derived by assuming CO line-luminosity ratios of  $\text{CO}(2-1)/\text{CO}(1-0) = 0.65$  and  $\text{CO}(3-2)/\text{CO}(1-0) = 0.55$ , which are typical values for local star-forming galaxies (e.g., Saintonge et al. 2017; Lamperti et al. 2020;

<sup>5</sup> A presentation of this work is found here: <https://www.youtube.com/watch?v=qz92y4AtpDo>.

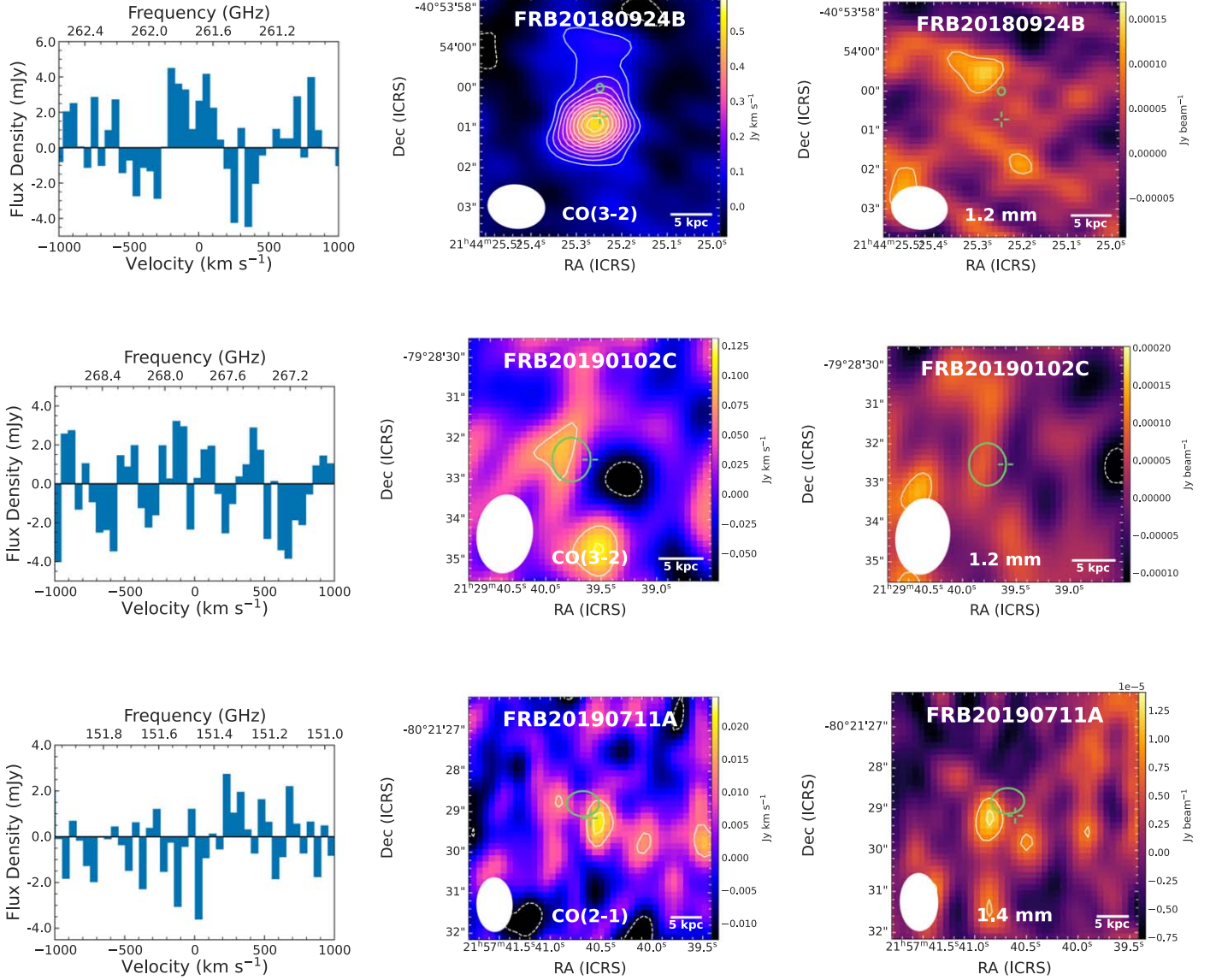


**Figure 1.** CO spectrum (left column), CO velocity-integrated intensity map (middle column), and continuum map (right column) of the host galaxies of FRB 20180924B (top row), FRB 20190102C (middle row), and FRB 20190711A (bottom row). The velocity resolution of the spectrum is  $50 \text{ km s}^{-1}$ , and the line flux is measured with a  $1''$ -radius aperture centered at the host-galaxy position. The velocity from  $-200$  to  $+200 \text{ km s}^{-1}$  is integrated for the velocity-integrated intensity maps of the hosts of FRBs 20180924B and 20190102C, while the range from  $+200$  to  $+400 \text{ km s}^{-1}$  is integrated for the FRB 20190711A host. The contours are  $\pm 2\sigma$ ,  $\pm 3\sigma$ , and a  $1\sigma$  step subsequently. The maximum contour level for the velocity-integrated intensity map of the FRB20180924A host is  $11\sigma$ . The green circle shows the 90% confidence region of the FRB position (Macquart et al. 2020). The green cross represents the host position (Heintz et al. 2020). The synthesized beam size is shown in the lower-left corner of the maps.

den Brok et al. 2021; Yajima et al. 2021). The conversion factor  $\alpha_{\text{CO}}$  is thought to be dependent on gas-phase metallicity, increasing  $\alpha_{\text{CO}}$  with decreasing metallicity (e.g., Bolatto et al. 2013). The Milky Way-like  $\alpha_{\text{CO}}$  of  $4.3 M_{\odot} (\text{K km s}^{-1} \text{pc}^2)^{-1}$  (Bolatto et al. 2013) is adopted for the hosts of FRBs 20180924B and 20190102C, where the gas-phase metallicity is comparable to that of the Milky Way. Because the metallicity of the FRB 20190711A host was not obtained from emission-line diagnostics, we derive the metallicity of  $12 + \log(\text{O}/\text{H}) = 8.3$  from the mass-metallicity relation of Genzel et al. (2015). The metallicity is lower than that of the Milky Way, and we adopt a metallicity-dependent  $\alpha_{\text{CO}}$ . There are many previous studies of the relation between metallicity and  $\alpha_{\text{CO}}$  (e.g., Wilson 1995; Genzel et al. 2012; Schruba et al. 2012; Bolatto et al. 2013). The relation of Genzel et al. (2012), where they use the samples of local

and high-redshift star-forming galaxies, gives  $\alpha_{\text{CO}}$  of  $8.9 M_{\odot} (\text{K km s}^{-1} \text{pc}^2)^{-1}$ . If we adopt the relation of Schruba et al. (2012) for nonstarburst galaxies, where they use the samples of nearby star-forming galaxies including low-metallicity dwarf galaxies, gives  $\alpha_{\text{CO}}$  of  $60 M_{\odot} (\text{K km s}^{-1} \text{pc}^2)^{-1}$ . To conservatively estimate an upper limit on molecular gas mass, we adopt  $\alpha_{\text{CO}} = 60 M_{\odot} (\text{K km s}^{-1} \text{pc}^2)^{-1}$  for the FRB 20190711A host. The molecular gas mass of the FRB 20180924B host is estimated to be  $(2.4 \pm 0.2) \times 10^9 M_{\odot}$ . The  $3\sigma$  upper limit for the hosts of FRBs 20190102C and 20190711A is  $< 3.8 \times 10^8 M_{\odot}$ , and  $< 1.2 \times 10^{10} M_{\odot}$  respectively, by assuming a line width of  $160 \text{ K km s}^{-1}$ , which is an average CO line width of nearby low-mass ( $10^{8.5} < M_{*}/M_{\odot} < 10^{10}$ ) star-forming galaxies in the ALLSMOG sample (Cicone et al. 2017). The results of ALMA observations on molecular gas are summarized in Table 1.



**Table 1**  
Results of CO ALMA Observations

FRB	CO <sup>a</sup>	Beam Size (arcseconds)	Rms <sup>b</sup> ( $\mu$ Jy beam <sup>-1</sup> )	$S_{\text{CO}}\Delta v^c$ (Jy km s <sup>-1</sup> )	$L'_{\text{CO}}^d$ (K km s <sup>-1</sup> pc <sup>2</sup> )
20180924B	3–2	1''43 × 1''09 (PA = +83°7)	34	0.50 ± 0.04	(3.1 ± 0.3) × 10 <sup>8</sup>
20190102C	3–2	1''94 × 1''37 (PA = -7°2)	340	<0.088	<4.9 × 10 <sup>7</sup>
20190711A	2–1	1''33 × 0''88 (PA = +0°8)	67	<0.017	<7.3 × 10 <sup>7</sup>

**Notes.** Limits are  $3\sigma$ .

<sup>a</sup> CO rotational transition.

<sup>b</sup> rms noise level with a velocity resolution of 50 km s<sup>-1</sup>.

<sup>c</sup> Velocity-integrated CO flux. A velocity width of 160 km s<sup>-1</sup> is assumed for nondetection.

<sup>d</sup> Line luminosity of CO(3–2) or CO(2–1).

**Table 2**  
Host-galaxy Properties

FRB	$M_{\text{gas}}^a$ ( $M_{\odot}$ )	References	$M_{\star}$ ( $M_{\odot}$ )	SFR ( $M_{\odot}$ yr <sup>-1</sup> )	References	$\mu_{\text{gas}}^b$ (Gyr)	$\tau_{\text{depl}}^c$ (Gyr <sup>-1</sup> )	SFE <sup>d</sup>
20121102A	$<9.1 \times 10^9$	1	$(1.4 \pm 0.7) \times 10^9$	$0.15 \pm 0.04$	4	65	<61	>0.017
20180924B	$(2.4 \pm 0.2) \times 10^9$	1	$(1.32 \pm 0.51) \times 10^{10}$	$0.88 \pm 0.26$	4	$0.18 \pm 0.07$	$2.8 \pm 0.8$	$0.36 \pm 0.11$
20190102C	$<3.8 \times 10^8$	1	$(3.39 \pm 1.02) \times 10^9$	$0.86 \pm 0.26$	4	<0.11	<0.45	>2.2
20190711A	$<6.7 \times 10^9$	1	$(8.1 \pm 2.9) \times 10^8$	$0.42 \pm 0.12$	4	<8.3	<16	>0.063
20200120E	$4 \times 10^7$	2	$(7.2 \pm 1.7) \times 10^{10}$	$0.6 \pm 0.2$	4	$(5.6 \pm 1.3) \times 10^{-4}$	$0.067 \pm 0.022$	$15 \pm 5$
20200428A	$2.5 \times 10^9$	3	$(6.08 \pm 1.14) \times 10^{10}$	$1.65 \pm 0.19$	5	$0.041 \pm 0.008$	$1.5 \pm 0.2$	$0.66 \pm 0.08$

**Notes.** Limits are  $3\sigma$ .

<sup>a</sup> Molecular gas mass derived with the Milky Way conversion factor ( $\alpha_{\text{CO}} = 4.3 M_{\odot}$  (K km s<sup>-1</sup> pc<sup>2</sup>)<sup>-1</sup>) except for the FRB 20121102A host ( $\alpha_{\text{CO}} = 200 M_{\odot}$  (K km s<sup>-1</sup> pc<sup>2</sup>)<sup>-1</sup>) and the FRB 20190711A host ( $\alpha_{\text{CO}} = 60 M_{\odot}$  (K km s<sup>-1</sup> pc<sup>2</sup>)<sup>-1</sup>).

<sup>b</sup> Molecular gas mass fraction ( $M_{\text{gas}}/M_{\star}$ ).

<sup>c</sup> Gas depletion time ( $M_{\text{gas}}/\text{SFR}$ ).

<sup>d</sup> Star formation efficiency ( $\text{SFR}/M_{\text{gas}}$ ).

**References.** (1) This work. (2) Brouillet et al. (1991). (3) Kalberla & Kerp (2009). (4) Heintz et al. (2020). (5) Licquia & Newman (2015).

### 3.2. Molecular Gas Properties

In addition to the FRB hosts observed by ALMA, we include three FRB hosts for which molecular gas information is available in the literature in the discussion to expand the sample size. The CO(1–0) and (3–2) observations of the FRB 20121102A host by Bower et al. (2018) provided  $3\sigma$  upper limits of  $L'_{\text{CO}(1-0)} < 2.3 \times 10^9$  K km s<sup>-1</sup> pc<sup>2</sup> and  $L'_{\text{CO}(3-2)} < 2.5 \times 10^8$  K km s<sup>-1</sup> pc<sup>2</sup>. The molecular gas mass of  $M_{\text{gas}} < 9.1 \times 10^9 M_{\odot}$  is derived from the CO(3–2) line luminosity by using the metallicity-dependent  $\alpha_{\text{CO}}$  of  $200 M_{\odot}$  (K km s<sup>-1</sup> pc<sup>2</sup>)<sup>-1</sup> (Schrubba et al. 2012) and the same CO line-luminosity ratio adopted for our sample. We also include two events: FRB 20200120E and FRB 20200428A. FRB 20200120E is the closest-known extragalactic FRB, localized to a globular cluster associated with M81 (Bhardwaj et al. 2021; Kirsten et al. 2022). FRB 20200428A was identified as the Galactic magnetar SGR 1935+2154 (Bochenek et al. 2020; The CHIME/FRB Collaboration et al. 2020). Since they occupy different positions on the phase space of luminosity and duration of FRBs, it is actively debated whether they are the same populations as other FRBs (e.g., Nimmo et al. 2022). Although the positions of the two nearby FRBs within the host galaxies are localized, we use the values for the entire host galaxies to treat them the same way as other FRBs. The host-galaxy properties are presented in Table 2.

We compare the molecular gas mass of the FRB hosts with SFR in Figure 2. We find that the FRB hosts have diversity in molecular gas properties. The hosts span a wide range in the

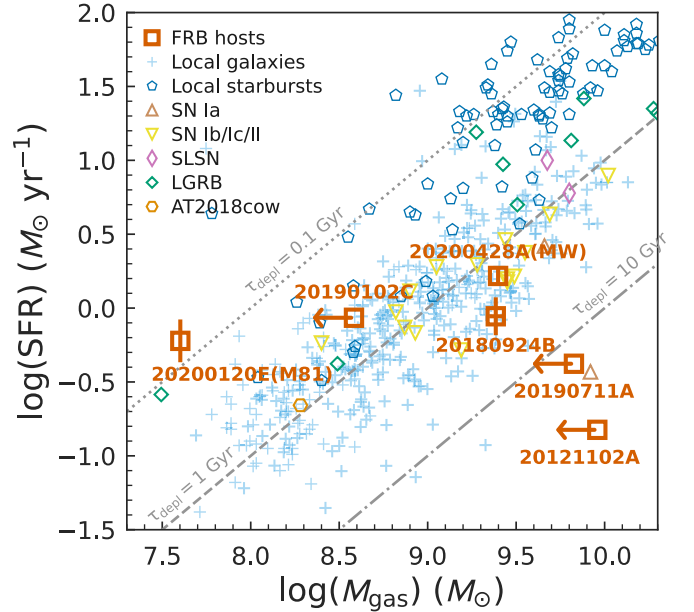


**Figure 2.** Comparison of molecular gas mass and SFR of the FRB hosts. For comparison, we plot local star-forming galaxies from the samples of ALLSMOG (Cicone et al. 2017) and xCOLDGASS (Saintonge et al. 2017), starbursts (Kennicutt & Reyes 2021), the hosts of SNe (Galbany et al. 2017), SLSNe (Arabsalmani et al. 2019; Hatsukade et al. 2020a), LGRBs (Hatsukade et al. 2020b), and AT2018cow (Morokuma-Matsui et al. 2019). The dotted, dashed, and dotted-dashed lines represent gas depletion times of 0.1, 1, and 10 Gyr, respectively.

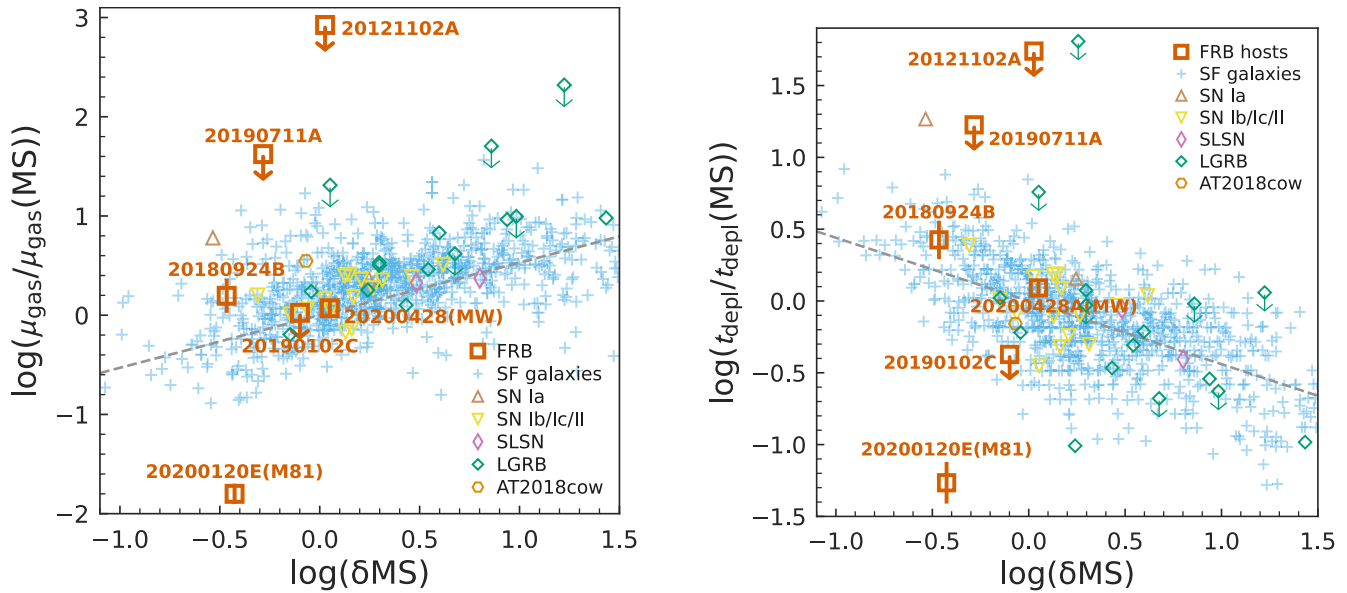


**Figure 3.** Molecular gas fraction (left) and gas depletion time (right) as a function of the offset from the reference MS line after removal of redshift dependence. For comparison, star-forming galaxies (Cicone et al. 2017; Tacconi et al. 2018) and the hosts of SNe (Galbany et al. 2017), SLSNe (Arabsalmani et al. 2019; Hatsukade et al. 2020a), LGRBs (Hatsukade et al. 2020b), and AT2018cow (Morokuma-Matsui et al. 2019) are presented. We restricted the redshift of the galaxies in the comparison to  $z < 1$  to match the redshift range of the FRB hosts. The dashed line shows the best-fit line for the MS galaxies derived in Tacconi et al. (2018).

plot with the molecular gas mass from  $4 \times 10^7 M_{\odot}$  to  $2.4 \times 10^9 M_{\odot}$  and the gas depletion time from 0.07 to 2.8 Gyr. While the FRB 20180924B host is molecular gas-rich compared to local star-forming galaxies, the hosts of FRBs 20190102C and 20200120E are molecular gas-poor for its SFR with a shorter gas depletion time.

The molecular gas mass fraction ( $\mu_{\text{gas}}$ ) and gas depletion time ( $\tau_{\text{gas}}$ ) depend on redshift, stellar mass, and offset from the main-sequence (MS) line (e.g., Genzel et al. 2015). Genzel et al. (2015) and Tacconi et al. (2018) argue that the parameter dependencies of  $\mu_{\text{gas}}$  and  $\tau_{\text{gas}}$  can be separated as products of power laws of redshift, offset from the MS line ( $\delta\text{MS} = \text{sSFR}/\text{sSFR}(\text{MS}, z, M_*)$ ), and stellar mass:  $\mu_{\text{gas}} \propto (1+z)^{2.5}(\delta\text{MS})^{0.52}(M_*)^{-0.36}$ ,  $\tau_{\text{gas}} \propto (1+z)^{-0.6}(\delta\text{MS})^{-0.44}$ . In Figure 3, we show  $\mu_{\text{gas}}$  and  $\tau_{\text{gas}}$  as a function of  $\delta\text{MS}$  after removing the above redshift dependence for each galaxy. We find that the FRB 20180924B host has a larger molecular gas fraction, and the FRB 20190102C host has a shorter gas depletion time for their stellar mass and SFR, deviating with  $>0.4$  dex from the scaling relations of other star-forming galaxies. The FRB 20200120E host has a smaller gas fraction and a shorter gas depletion time and is largely offset from the distributions of other star-forming galaxies. Those FRB hosts are offset from the scaling relations of other star-forming galaxies, which is in contrast to the majority of the hosts of core-collapse SNe, SLSNe (Hatsukade et al. 2020a), and LGRBs (Hatsukade et al. 2020b), suggesting different origins of FRBs. The small sample size also prevents us from discussing the difference between repeating and nonrepeating FRBs, leaving it for future works.

To discuss the statistical significance of the difference between the FRB hosts and normal star-forming galaxies, we compare with the ALLSMOG sample (Cicone et al. 2017). The sample consists of star-forming galaxies at  $0.01 < z < 0.03$  with stellar masses in the range  $8.5 < \log(M_*/M_{\odot}) < 10$ , which matches to the mass range of our FRB host sample. Because the redshift distribution differs between the two samples, we remove the redshift dependence of  $\mu_{\text{gas}}$  and  $\tau_{\text{depl}}$  by using the prescription of

Tacconi et al. (2018) as stated above. To take into account nondetections in the samples, we adopt the Kaplan–Meier estimator (Kaplan & Meier 1958), a nonparametric statistic to estimate the probability distribution of data containing nondetections. We applied this analysis to  $\mu_{\text{gas}}$  and  $\tau_{\text{depl}}$  using a Python package `lifelines` (Davidson-Pilon 2019). The log-rank test shows a  $p$ -value of 0.048 and 0.83 for  $\mu_{\text{gas}}$  and  $\tau_{\text{depl}}$ , respectively, suggesting a difference in the distribution of  $\mu_{\text{gas}}$  between the two samples. If we remove an outlier, the FRB 20200120E host, it becomes inconclusive with a  $p$ -value of 0.19, and a larger sample is required to test the difference.

We also conduct the same analysis with the hosts of core-collapse SNe (Galbany et al. 2017), and no statistically significant results are obtained.

#### 4. Conclusions and Implication for Progenitors

In this study, we report molecular gas properties of six FRB hosts obtained from ALMA observations (20180924B, 20190102C, and 20190711A) and in the literature (20121102A, 20200120E, and 20200428A), allowing comparisons of a sample of FRB hosts with other galaxy populations for the first time. We found the diversity of molecular gas properties of the FRB hosts with wide ranges of molecular gas mass, gas depletion time, and gas mass fraction. Compared to other star-forming galaxy populations, the FRB 20180924B host is molecular gas-rich, and the hosts of FRBs 20190102C and 20200120E are molecular gas-poor with a shorter gas depletion for their stellar mass and SFR.

Optical studies found various properties in FRB hosts, such as morphologies, colors, luminosities, stellar masses, SFRs, ages, or emission-line ratios in the BPT diagram, and they do not track the distribution of field galaxies (e.g., Heintz et al. 2020; Bhandari et al. 2022). Our study adds a new perspective of molecular gas to the diversity of FRB hosts. If FRBs originate from massive stars (similar to core-collapse SNe or LGRBs) or their remnants, an adequate quantity of molecular gas is expected for producing the progenitors. In contrast, less

molecular gas is expected in such environments if FRBs originate from old populations (such as white dwarfs, old neutron stars, and stellar-mass black holes). Although we cannot constrain specific progenitor models, our findings suggest that FRBs arise from multiple progenitors or from a single progenitor that can exist in a wide range of host-galaxy environments.

Currently, the limited sample size makes statistical comparisons with other galaxy environments difficult. Ongoing and future molecular gas observations will overcome this situation as the number of detected FRBs and their localized host galaxies rapidly increases. In addition, it is essential to spatially resolve the host galaxies to determine the nature of the molecular gas at the FRB positions in detail. This would help settle the debate over whether the progenitors of FRBs are old populations or not.

We would like to acknowledge the reviewers for helpful comments and suggestions which significantly improved the Letter. We thank ALMA staff for data acquisition. B.H. is supported by JSPS KAKENHI grant No. 19K03925. T.H. acknowledges the supports of the Ministry of Science and Technology of Taiwan through grants 110-2112-M-005-013-MY3, 110-2112-M-007-034-, and 111-2123-M-001-008-. T.-Y.H. is supported by the University Consortium of ALMA-Taiwan Center for ALMA Science Advancement through a grant 110-2112-M-007-034-. This work is supported by the ALMA Japan Research Grant of NAOJ Chile Observatory (NAOJ-ALMA-268). This paper makes use of the following ALMA data: ADS/JAO.ALMA#2021.1.00027.S and #2019.1.01450.S. ALMA is a partnership of ESO (representing its member states), NSF (USA) and NINS (Japan), together with NRC (Canada), MOST and ASIAA (Taiwan), and KASI (Republic of Korea), in cooperation with the Republic of Chile. The Joint ALMA Observatory is operated by ESO, AUI/NRAO and NAOJ.

*Facility:* ALMA.

*Software:* CASA (McMullin et al. 2007), ASTROPY (The Astropy Collaboration et al. 2013, 2018).

### ORCID iDs

Bunyo Hatsukade  <https://orcid.org/0000-0001-6469-8725>  
 Tetsuya Hashimoto  <https://orcid.org/0000-0001-7228-1428>  
 Yuu Niino  <https://orcid.org/0000-0001-5322-5076>  
 Tzu-Yin Hsu  <https://orcid.org/0000-0002-0944-5634>

### References

Arabsalmani, M., Roychowdhury, S., Renaud, F., et al. 2019, *ApJ*, 882, 31  
 Baldwin, J. A., Phillips, M. M., & Terlevich, R. 1981, *PASP*, 93, 5

Bannister, K. W., Deller, A. T., Phillips, C., et al. 2019, *Sci*, 365, 565  
 Bhandari, S., Heintz, K. E., Aggarwal, K., et al. 2022, *AJ*, 163, 69  
 Bhandari, S., Sadler, E. M., Prochaska, J. X., et al. 2020, *ApJL*, 895, L37  
 Bhardwaj, M., Gaensler, B. M., Kaspi, V. M., et al. 2021, *ApJL*, 910, L18  
 Bochenek, C. D., Ravi, V., Belov, K. V., et al. 2020, *Natur*, 587, 59  
 Bolatto, A. D., Warren, S. R., Leroy, A. K., et al. 2013, *Natur*, 499, 450  
 Bower, G. C., Rao, R., Krips, M., et al. 2018, *AJ*, 155, 227  
 Brouillet, N., Baudry, A., Combes, F., Kaufman, M., & Bash, F. 1991, *A&A*, 242, 35  
 Chabrier, G. 2003, *PASP*, 115, 763  
 Chatterjee, S., Law, C. J., Wharton, R. S., et al. 2017, *Natur*, 541, 58  
 Cicone, C., Bothwell, M., Wagg, J., et al. 2017, *A&A*, 604, A53  
 Cordes, J. M., & Chatterjee, S. 2019, *ARA&A*, 57, 417  
 Davidson-Pilon, C. 2019, *JOSS*, 4, 1317  
 den Brok, J. S., Chatzigiannakis, D., Bigiel, F., et al. 2021, *MNRAS*, 504, 3221  
 Galbany, L., Mora, L., González-Gaitán, S., et al. 2017, *MNRAS*, 468, 628  
 Genzel, R., Tacconi, L. J., Combes, F., et al. 2012, *ApJ*, 746, 69  
 Genzel, R., Tacconi, L. J., Lutz, D., et al. 2015, *ApJ*, 800, 20  
 Hashimoto, T., Goto, T., Wang, T.-W., et al. 2020, *MNRAS*, 494, 2886  
 Hashimoto, T., Hatsukade, B., Goto, T., et al. 2019, *MNRAS*, 488, 5029  
 Hatsukade, B., Morokuma-Matsui, K., Hayashi, M., et al. 2020a, *PASJ*, 72, L6  
 Hatsukade, B., Ohta, K., Hashimoto, T., et al. 2020b, *ApJ*, 892, 42  
 Heintz, K. E., Prochaska, J. X., Simha, S., et al. 2020, *ApJ*, 903, 152  
 Johnston, S., Taylor, R., Bailes, M., et al. 2008, *ExA*, 22, 151  
 Kalberla, P. M., & Kerp, J. 2009, *ARA&A*, 47, 27  
 Kaplan, E. L., & Meier, P. 1958, *J. Am. Stat. Assoc.*, 53, 457  
 Kennicutt, R. C., & Reyes, M. A. C. D. L. 2021, *ApJ*, 908, 61  
 Kirsten, F., Marcote, B., Nimmo, K., et al. 2022, *Natur*, 602, 585  
 Lamperti, I., Saintonge, A., Koss, M., et al. 2020, *ApJ*, 889, 103  
 Le Floch, E., Charmandaris, V., Forrest, W. J., et al. 2006, *ApJ*, 642, 636  
 Li, Y., & Zhang, B. 2020, *ApJL*, 899, L6  
 Li, Y., Zhang, B., Nagamine, K., & Shi, J. 2019, *ApJL*, 884, L26  
 Licquia, T. C., & Newman, J. A. 2015, *ApJ*, 806, 96  
 Macquart, J.-P., Prochaska, J. X., McQuinn, M., et al. 2020, *Natur*, 581, 391  
 Marcote, B., Nimmo, K., Hessels, J. W. T., et al. 2020, *Natur*, 577, 190  
 McMullin, J. P., Waters, B., Schiebel, D., Young, W., & Golap, K. 2007, in ASP Conf. Ser. 376, *Astronomical Data Analysis Software and Systems XVI*, ed. R. A. Shaw et al. (San Francisco, CA: ASP), 127  
 Morokuma-Matsui, K., Morokuma, T., Tominaga, N., et al. 2019, *ApJL*, 879, L13  
 Niino, Y., Aoki, K., Hashimoto, T., et al. 2017, *PASJ*, 69, 27  
 Nimmo, K., Hewitt, D. M., Hessels, J. W. T., et al. 2022, *ApJL*, 927, L3  
 Perley, D. A., Krühler, T., Schulze, S., et al. 2016, *ApJ*, 817, 7  
 Planck Collaboration, Aghanim, N., Akrami, Y., et al. 2020, *A&A*, 641, A6  
 Platts, E., Weltman, A., Walters, A., et al. 2019, *PhR*, 821, 1  
 Pleunis, Z., Good, D. C., Kaspi, V. M., et al. 2021, *ApJ*, 923, 1  
 Prochaska, J. X., Macquart, J.-P., McQuinn, M., et al. 2019, *Sci*, 366, 231  
 Saintonge, A., Catinella, B., Tacconi, L. J., et al. 2017, *ApJS*, 233, 22  
 Schruha, A., Leroy, A. K., Walter, F., et al. 2012, *AJ*, 143, 138  
 Solomon, P., & Vanden Bout, P. 2005, *ARA&A*, 43, 677  
 Tacconi, L. J., Genzel, R., Saintonge, A., et al. 2018, *ApJ*, 853, 179  
 The Astropy Collaboration, Price-Whelan, A. A. M., SipHocz, B. M., et al. 2018, *AJ*, 156, 123  
 The Astropy Collaboration, Robitaille, T. P., Tollerud, E. J., et al. 2013, *A&A*, 558, A33  
 The CHIME/FRB Collaboration, Andersen, B. C., Bandura, K. M., et al. 2020, *Natur*, 587, 54  
 Wilson, C. D. 1995, *ApJL*, 448, L97  
 Yajima, Y., Sorai, K., Miyamoto, Y., et al. 2021, *PASJ*, 73, 257